Fragmentation of percolation cluster perimeters

1996 J. Phys. A: Math. Gen. 29 2337

(http://iopscience.iop.org/0305-4470/29/10/013)

J. Phys. A: Math. Gen. **29** (1996) 2337–2348. Printed in the UK

Fragmentation of percolation cluster perimeters

Jean-Marc Debierre† and R Mark Bradley‡

† Laboratoire MATOP§, Case 151, Faculté des Sciences et Techniques de Saint-Jérôme, 13397 Marseille Cedex 20, France

‡ Department of Physics, Colorado State University, Fort Collins, CO 80523, USA

Received 3 August 1995, in final form 12 February 1996

Abstract. We introduce a model for the fragmentation of porous random solids under the action of an external agent. In our model, the solid is represented by a bond percolation cluster on the square lattice and bonds are removed only at the external perimeter (or 'hull') of the cluster. This model is shown to be related to the self-avoiding walk on the Manhattan lattice and to the disconnection events at a diffusion front. These correspondences are used to predict the leading and the first correction-to-scaling exponents for several quantities defined for hull fragmentation. Our numerical results support these predictions. In addition, the algorithm used to construct the perimeters reveals itself to be a very efficient tool for detecting subtle correlations in the pseudo-random number generator used. We present a quantitative test of two generators which supports recent results reported in more systematic studies.

1. Introduction

Many porous solids (such as silica aerogels, sintered materials, and some types of sandstone and charcoal) are only tenuously connected and thus fragment easily. The structure of these solids usually involves a high degree of randomness. Percolation clusters are the simplest random, porous objects. With this motivation, Gyure, Edwards and Ferer (GEF) recently studied the fragmentation of bond percolation clusters on the square lattice [1]. In their work, a single bond was removed at a randomly chosen point within the cluster. If fragmentation occurred, the sizes of the daughter clusters were recorded. Ultimately, GEF studied the scaling properties of the fragment size distribution. GEF's model is believed to capture some of the essential features of the fragmentation of real porous solids.

Real porous solids can fragment during etching by a chemical agent or during combustion. In both instances, material is removed only at the external surface of the porous solid. In GEF's model, however, a bond is removed at any point within the cluster. Therefore, their model should not be applied to the combustion or etching of porous materials.

To obtain a model for these phenomena, in this paper we will modify GEF's model so that bonds are removed only on the external surface (or 'hull') of the percolation cluster. Since the hull and bulk properties differ for two-dimensional percolation clusters [2], we expect that the scaling properties of the two models of fragmentation will also differ. Specifically, we study the fragmentation of the external perimeters of critical bond percolation clusters on the square lattice. We present the results of intensive numerical simulations in which the perimeters are first constructed and then fragmented exhaustively. The size distribution of

† Unité de Recherche Associée au CNRS 1530.

0305-4470/96/102337+12$19.50

the constructed perimeters is used for testing our algorithm. This test reveals the existence of a subtle bias in a widely used random number generator, R250.

We establish connections between the fragmentation of the external perimeters and two other statistical models: the self-attracting self-avoiding loop on the Manhattan lattice [3] and the temporal fluctuations of a diffusion front [4]. This allows us to make very precise predictions for the scaling form of various physical quantities. The behaviour of the leading-order and first correction terms are checked numerically in each case and very good agreement is found with the expected behaviour. Our results allow us to find the first accurate estimate for the exponent associated with the hull fragment size distribution. Finally, a number of scaling prefactors are also estimated.

The paper is organized as follows. The model and the algorithm used in the simulations are described in section 2. Section 3 deals with the relations of hull fragmentation to the two problems mentioned in the previous paragraph. The results for the perimeter size distribution are presented in section 4, and section 5 concerns our results on hull fragmentation. Finally, section 6 summarizes the results obtained in the paper.

2. The model

Consider bond percolation on a square lattice with lattice spacing a at the percolation threshold $p = p_c = \frac{1}{2}$. Each cluster has a single external perimeter (its 'hull'), and it may have no internal perimeters or a number of them. To construct the percolation cluster perimeters without constructing the clusters themselves, we use a hull-generating walk [5] introduced by Gunn and Ortuño [6].

The Gunn and Ortuño walk (GOW) is a random walk on the covering lattice of the original square lattice (figure 1). (The covering lattice is a square lattice obtained by joining the centres of adjacent bonds on the original lattice.) We will set $a = \sqrt{2}$, so that the bonds on the covering lattice have unit length. Initially, the states of all the bonds on the original lattice are unspecified, i.e. they are neither occupied nor vacant. The walk starts at the origin of the covering lattice. At the first time step, one of the four possible directions

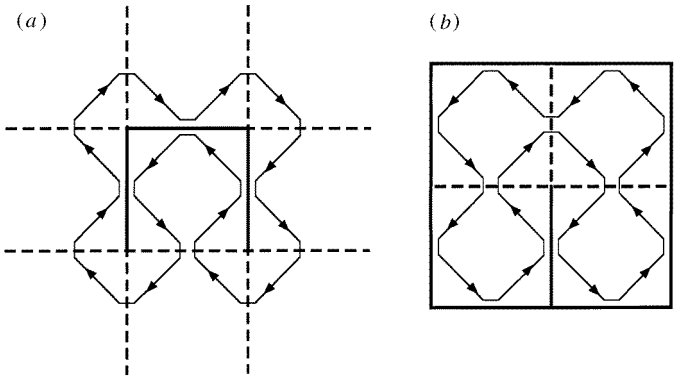

Figure 1. Two 16-step GOW (thin lines) and the corresponding percolation cluster perimeters. (*a*) The external perimeter is made up of three occupied bonds (bold lines), plus nine vacant bonds (broken lines). There are four constriction points and three fragmenting bonds on this perimeter. (*b*) The internal perimeter is made up of nine occupied bonds (bold lines), plus three vacant bonds (broken lines). There are four constriction points and one fragmenting bond on this perimeter.

is randomly chosen and a unit step is performed in this direction. The bond reached by the walk is called the target bond. The GOW is then constructed step by step. At each step, the nature of the target bond is tested. If its state has not yet been specified, it becomes occupied or vacant with equal probability. On the other hand, if the state of the target bond has previously been designated, its state is left unchanged. The next step is to the right if the target bond is vacant and to the left if it is occupied. The walk stops when it attempts to re-traverse the initial step. It is then a closed loop.

It is straightforward to see that the GOW generates a perimeter of a percolation cluster at $p = p_c = \frac{1}{2}$. With our conventions, GOWs that close in a clockwise fashion are external perimeters, while GOWs that close in a counterclockwise fashion are internal perimeters.

We now restrict our attention to the external perimeters generated by the GOW. The occupied bonds on the original lattice that are touched by the GOW are the hull bonds. One of these hull bonds is now chosen at random and is replaced by an unoccupied bond. This combustion (or chemical etching) event may or may not result in the fragmentation of the percolation cluster. In this paper, we will remove a single hull bond and study the resulting fragments. Therefore, our work concerns only the initial stages of the fragmentation process (the same is true of the work of GEF).

A *fragmenting bond* will be defined to be an occupied bond on the original lattice that the GOW visits twice (see figure 1). The removal of the chosen bond only results in the fragmentation of the percolation cluster if the chosen bond is a fragmenting bond. If the chosen bond is indeed a fragmenting bond, the GOW is modified to reflect the fact that the chosen bond is now unoccupied (see figure 2). This results in the fragmentation of the parent GOW into two loops that trace out the perimeters of the cluster fragments.

Suppose that the original GOW of s steps is fragmented into two loops of s' and $s - s'$ steps, respectively, and let $s' \leqslant s - s'$, so that the loop of s' steps is the smaller of the two fragments. We define $P_{s',s}$ to be the probability that a daughter GOW of s' steps is obtained from the combustion of a parent loop of length s. Note that the probability that combustion actually fragments a GOW of s steps, $P_f(s) \equiv \sum_{s'=4}^{s/2} P_{s',s}$, is in general different from unity.

In our simulations, the GOWs were generated on a $65\,536 \times 65\,536$ square lattice. This lattice was divided into cells of size 256×256 and memory was only allocated to the cells visited by the walk. This data-blocking technique has proven to be a very efficient tool for constructing hull-generating walks [2, 7]. Since the walks were also fragmented in our simulations, memory had to be allocated as efficiently as possible. A bit-coding technique was therefore used to store the visited cells. The construction of a GOW was terminated if the number of steps performed exceeded a cut-off value $s_{max} = 2^{20}$. With this cut-off, the boundaries of the lattice were never reached and it appeared to be virtually infinite.

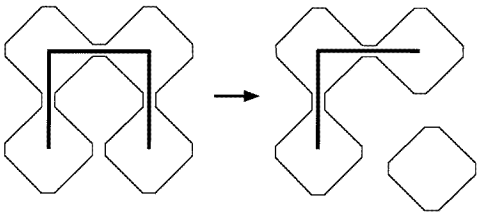

Figure 2. Fragmentation of a 16-step GOW into a 12-step and a 4-step GOW (thin lines). For clarity, we have only shown the occupied bonds (bold lines) in the corresponding percolation perimeters. The fragmentation is caused by the removal of the right vertical occupied bond in the original perimeter.

During the construction of a perimeter, each time a new step was made, the target bond was tagged by an integer value equal to the total number of steps performed up until that point. Thus, fragmenting bonds were assigned two tags whose difference gave the number of steps in one of the two corresponding fragments. When a perimeter closed after s steps, each pair of fragments with lengths $s - s'$ and s' associated with a given fragmenting bond was examined and only the smaller fragment was kept in memory. We were able to perform this task efficiently by using a hash list to store the coordinates of the visited bonds. In this paper, only the data we obtained for fragmentation of external perimeters will be discussed.

3. Relationship of hull fragmentation to two other models

As mentioned in the introduction, hull fragmentation is related to two other models. We will begin by discussing the relation to self-attracting self-avoiding loops on the Manhattan lattice.

Let us define a *constriction point* to be any point that is touched twice by the GOW (see figure 1). A constriction point can lie at the centre of either an occupied or a vacant bond. If a constriction point lies at the centre of an occupied bond, the bond is a fragmenting bond. An unoccupied bond with a constriction point at its centre will be called a *non-fragmenting bond*. We will denote the number of constriction points, fragmenting bonds, and non-fragmenting bonds touched by a clockwise GOW of s steps by $N_{\mathrm{c}}(s)$, $N_{\mathrm{f}}(s)$ and $N_{\mathrm{n}}(s)$, respectively. Clearly, $N_{\mathrm{c}}(s) = N_{\mathrm{f}}(s) + N_{\mathrm{n}}(s)$.

A closed Gunn and Ortuño walk can be mapped onto the self-attracting self-avoiding loop on the Manhattan lattice at its theta point (θ-MSASAL) [3]. A number of exact results are known for the latter model (for a recent review, see [8]). In particular, the average energy of a θ-MSASAL of s steps scales as $\frac{2}{3}\epsilon s + 2\epsilon A s^{3/7}$ as s tends to infinity. Here ϵ is the energy assigned to each unbonded nearest-neighbour pair and A is a non-zero constant. Under the mapping, a θ-MSASAL with s steps and energy $2\epsilon N$ is transformed into a GOW with s steps and N constriction points. Thus, the average number of constriction points in a GOW of s steps scales as $\frac{1}{3}s + As^{3/7}$.

This result applies to GOWs of s steps that close in either a clockwise or counterclockwise fashion. However, simply by reversing the direction of the walk, any clockwise GOW can be converted into a counterclockwise GOW, and vice versa. As a result, the average number of constriction points on a clockwise GOW of s steps, $\langle N_{\mathrm{c}}(s)\rangle$, scales as

$$\langle N_{\mathrm{c}}(s)\rangle \simeq \tfrac{1}{3}s + As^{3/7}\,. \tag{3.1}$$

Let π_s^+ (π_s^-) be the probability that a hull-generating walk closes in exactly s steps in a clockwise (counterclockwise) fashion. Ziff has argued that there is a symmetry about the percolation threshold, and, consequently, π_s^+/π_s^- should tend to 1 as s tends to infinity for $p = p_{\mathrm{c}}$ [2]. Using this as a criterion to locate the percolation threshold for site percolation on the square lattice, Ziff obtained an extremely accurate value for p_{c} that is in accord with estimates obtained by other means.

The GOW generates a perimeter of a bond percolation cluster on the square lattice at the percolation threshold. Therefore, if Ziff's conjecture is valid, π_s^+/π_s^- should tend to 1 as s tends to infinity. We now make an analogous conjecture. Let the mean number of fragmenting bonds touched by *counterclockwise* GOWs of s steps be denoted by $\langle N_{\mathrm{f}}'(s)\rangle$. We conjecture that

$$\frac{\langle N_{\mathrm{f}}'(s)\rangle}{\langle N_{\mathrm{f}}(s)\rangle} \to 1 \qquad \text{as} \quad s \to \infty\,. \tag{3.2}$$

A clockwise GOW traces out the external perimeter of a percolation cluster. If the direction of this GOW is reversed, it becomes a counterclockwise GOW that generates the internal perimeter of a percolation cluster. Under this reversal, the clockwise GOWs non-fragmenting bonds become the fragmenting bonds of the counterclockwise GOW (figure 1). Therefore, $N_n(s) = N'_f(s)$, and equation (3.2) becomes

$$\frac{\langle N_n(s)\rangle}{\langle N_f(s)\rangle} \to 1 \qquad \text{as} \quad s \to \infty . \tag{3.3}$$

As we shall see in section 5, our Monte Carlo results are in excellent agreement with this conjecture, and we now presume equation (3.3) to be valid. Since

$$\langle N_f(s)\rangle + \langle N_n(s)\rangle = \langle N_c(s)\rangle$$

equation (3.1) then shows that both $\langle N_f(s)\rangle/s$ and $\langle N_n(s)\rangle/s$ must tend to $\frac{1}{6}$ as s tends to infinity. Moreover, as $s \to \infty$, we must have

$$\langle N_f(s)\rangle \simeq \tfrac{1}{6}s + A_f s^{3/7} \tag{3.4}$$

and

$$\langle N_n(s)\rangle \simeq \tfrac{1}{6}s + A_n s^{3/7} \tag{3.5}$$

where $A_f + A_n = A$. There is no reason to assume that A_f and A_n are equal, and our Monte Carlo results strongly suggest that they are not. Note that for large s, both $\langle N_f(s)\rangle$ and the number of occupied bonds touched by the GOW scale as s^1. Therefore, $P_f(s)$ tends to a non-zero constant as $s \to \infty$.

We now turn to the relation of our model to the problem studied by Gouyet and Boughaleb (GB) [4]. GB studied the diffusion of a set of non-interacting particles in the presence of a concentration gradient in the strip $\{(x, y) \mid 0 \leqslant x \leqslant L' \text{ and } 0 \leqslant y \leqslant L\}$. The length of the strip L' is assumed to be large compared to the width L, and $L \gg a$. The concentration of diffusers p is fixed at one for $x = 0$ and at zero for $x = L'$. This problem is also known as 'gradient percolation' since at any time the problem is equivalent to site percolation in which the fraction of occupied sites p varies linearly from one end of the strip to the other†. Naturally, there is a large cluster of particles that has one edge on the end of the strip with concentration $p = 1$. We will call this cluster the 'parent cluster'. The frontier of the parent cluster within the strip is called the diffusion front. Since the particles are all diffusing, the diffusion front is constantly fluctuating, and small clusters are continually joining and separating from the parent cluster at the diffusion front. It is these fluctuations that GB chose to study.

GB obtained a number of interesting results, but only one is of interest here. Let $N_{\text{frag}}(\sigma)$ be the number of clusters with an external perimeter of length σ that disconnect from the parent cluster in a unit time. GB argued that $N_{\text{frag}}(\sigma)$ follows the scaling form

$$N_{\text{frag}}(\sigma) = L\sigma^{-11/7}|\nabla p|^{-3/7} F(\sigma|\nabla p|) \tag{3.6}$$

where $|\nabla p| = 1/L'$ is the concentration gradient and F is a scaling function. Note that $F(0)$ is a finite, non-zero constant and that $F(x) \to 0$ as $x \to \infty$. Let $P_{\text{frag}}(\sigma)\Delta y$ be the

† Gradient percolation was first studied by Sapoval and co-workers [9].

probability that an external perimeter of length σ is disconnected from the parent cluster per unit time within the strip $\{(x, y) \mid 0 \leqslant x \leqslant L'$ and $y_0 \leqslant y \leqslant y_0 + \Delta y\}$. Here y_0 is a constant lying between zero and L and $a \ll \Delta y \ll L$. Clearly,

$$P_{\text{frag}}(\sigma) = \sigma^{-11/7} |\nabla p|^{-3/7} F(\sigma |\nabla p|) \,. \tag{3.7}$$

If $\sigma \ll |\nabla p|^{-1}$, then $P_{\text{frag}}(\sigma)$ scales as $\sigma^{-11/7}$ as a function of σ. On length scales small compared to the width of the diffusion front $w \sim |\nabla p|^{-4/7}$, the diffusion front has the same geometry as the infinite percolation cluster at threshold in percolation without a concentration gradient [4]. Therefore, $P_{\sigma,s} \sim \sigma^{-11/7}$ for $\sigma \ll s$. Now a fragment cannot have a perimeter longer than its parent, which means that this scaling behaviour must be cut off when σ approaches s. We conclude that $P_{\sigma,s}$ obeys the scaling law

$$P_{\sigma,s} \simeq \sigma^{-11/7} G(\sigma/s) \tag{3.8}$$

where the scaling function $G(x)$ is finite and non-zero for $x = 0$ and is zero for $x \geqslant 1$.

4. Monte Carlo results on the perimeter distribution

The first part of our algorithm, i.e. the construction of a percolation-cluster perimeter by a GOW, was tested before fragmentation was studied. We generated a total of 2×10^5 GOWs with a cut-off length of $s_{\max} = 2^{20}$. The number N_s^{ext} of external perimeters that closed after exactly s steps was computed. We also found the number of internal perimeters that closed after s steps, N_s^{int}. Due to the symmetry about p_c, the ratio $\rho_s \equiv N_s^{\text{ext}}/N_s^{\text{int}}$ should be equal to one at the percolation threshold [2, 7]. The ρ_s values obtained with two different pseudo-random number generators are displayed in figure 3. We have also shown error bars $\pm\Delta\rho_s$ approximately corresponding to one standard deviation, i.e. $\Delta\rho_s = 1/\sqrt{N_s^{\text{ext}}} + 1/\sqrt{N_s^{\text{int}}}$. The first generator (which is usually called R250 in the literature) is based on a generalized feedback shift register method. The ρ values obtained with R250 reveal significant correlations in this generator for $s > s_c = 300$–400. This is in good agreement with recent numerically intensive studies [10] that have shown that correlations can reveal themselves in R250 when more than 250 consecutive random numbers are used in a row for the same task. Our estimate for s_c is slightly higher than 250. This is because the GOW revisits roughly $\frac{1}{3}$ of the total number of bonds on average, as explained in the previous section. Thus, only 250 independent bonds are needed to construct a walk of $s \cong 375$ steps, a value in good agreement with our s_c estimate. Figure 3 also shows that the bias introduced by R250 favours internal perimeters for intermediate values of s and external perimeters for large values of s.

The second generator we used is a linear congruential generator with shuffling named RAN1 [11]. In contrast to R250, no bias was observed in the data obtained using RAN1 (figure 3). Accordingly, all subsequent calculations were made with this generator. To improve the statistics, the number of GOWs generated with RAN1 and $s_{\max} = 2^{20}$ was increased to 10^6. Generating and fragmenting these walks on an HP730 workstation required approximately 15 CPU days and 20 MB of memory.

A second test of our algorithm was obtained by checking the scaling of the distribution of walk lengths. Let the total number of GOWs that close after exactly s steps be N_s. Because the GOW generates the perimeter of a percolation cluster, N_s scales as

$$N_s \sim s^{1-\tau'} \tag{4.1}$$

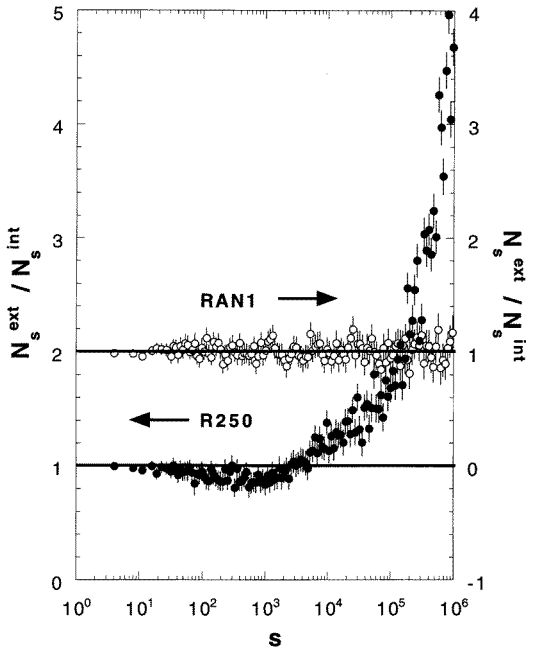

Figure 3. The number of external versus internal s-step perimeters as a function of s. The full (open) circles correspond to 2×10^5 perimeters constructed with the random number generator named R250 (RAN1).

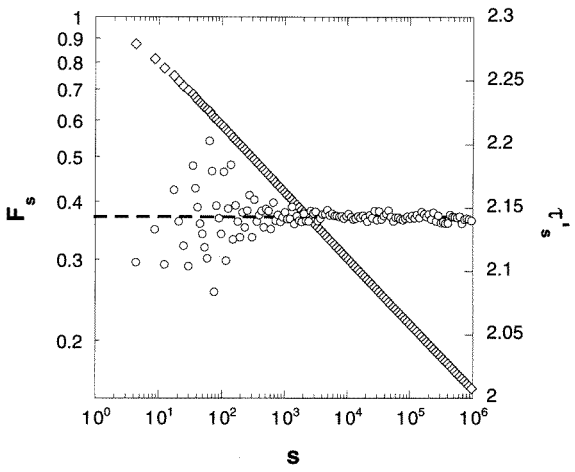

Figure 4. Computed fraction F_s of the GOWs that remain open after s steps (diamonds). Also shown is the finite-size estimator τ'_s (circles) which is deduced from the local slope $\Delta(\log F_s)/\Delta(\log s)$ for consecutive pairs of points. The broken line is the expected asymptotic value $\tau' = \frac{15}{7}$.

where the distribution exponent τ' is known to be exactly equal to $\frac{15}{7} = 2.142\,857\ldots$ [2, 12]. Accordingly, the fraction F_s of perimeters that are still open after s steps must scale as $s^{2-\tau'}$. Our data for F_s are plotted on logarithmic scales in figure 4. The local slope $\Delta(\log F_s)/\Delta(\log s)$ for consecutive pairs of points is used to compute a finite-size estimator τ'_s for exponent τ'. The fluctuations in τ'_s for small s are an artefact of our binning procedure (see section 5). τ'_s is roughly constant when $s > 10^3$ and its average value is found to be $\tau' = 2.1430 \pm 0.0003$ in this range. This is the most precise numerical estimate obtained for this exponent to date, and our value is in excellent accord with the exact result $\tau' = \frac{15}{7}$. This result strongly suggests that the correlations in RAN1 have a negligible effect on the results reported in the following section.

5. Monte Carlo simulations of hull fragmentation

The 422 201 clockwise GOWs that closed before reaching the maximum number of steps $s_{\max} = 2^{20}$ were taken into account in the fragmentation statistics. These are the external perimeters. The open walks and internal perimeters that were constructed were simply discarded. For the s-step external perimeters, we computed $\langle N_{\rm f}(s)\rangle$, $\langle N_{\rm c}(s)\rangle$, and the average number of fragmenting bonds whose removal would result in the formation of a daughter loop of s' steps, $F_{s',s}$. Note that $F_{s',s} = \langle N_{\rm f}(s)\rangle P_{s',s}/P_{\rm f}(s)$. The first moment of $F_{s',s}$ was calculated for the smaller fragments: i.e. we computed

$$M_1(s) \equiv \sum_{s'=4}^{s'=s/2} s' F_{s',s}\,. \tag{5.1}$$

The lower limit for this summation, $s' = 4$, corresponds to the smallest fragment that can be produced by removing a fragmenting bond in a GOW (see figure 2). From equations (3.4) and (3.8), we deduce that for large s

$$M_1(s) \simeq A' s^{10/7} + B' s \tag{5.2}$$

where the second term is an analytical correction due to the non-zero lower limit in (5.1).

To avoid large fluctuations, we binned our data for $\langle N_{\rm f}(s)\rangle$, $\langle N_{\rm c}(s)\rangle$ and $M_1(s)$ in much the same way as GEF did. The bins, which are numbered with the positive integer value i, were defined to be the set of intervals $s \in [4\alpha^{i-1}, 4\alpha^i)$ with $\alpha = 2^{1/8}$. For instance, the binned average number of fragmenting bonds, Φ_s, was defined as follows:

$$\Phi_s = \left(\sum_{\sigma=s}^{\sigma=\alpha s} N_\sigma\right)^{-1} \sum_{\sigma=s}^{\sigma=\alpha s} \langle N_{\rm f}(\sigma)\rangle N_\sigma \tag{5.3}$$

where N_σ is the number of σ-step external perimeters constructed. Similar expressions were used to calculate Ω_s and μ_s, the binned quantities for the average number of constriction points $\langle N_{\rm c}(s)\rangle$ and for the first moment $M_1(s)$, respectively.

This binning procedure changes the values of the constants appearing in equations (3.1), (3.4) and (5.2). Combining (3.4), (4.1) and (5.3) and restricting the calculation to the two leading terms, we obtain

$$\Phi_s \simeq \frac{s}{6}\left[\left(\frac{2-\tau'}{3-\tau'}\right)\left(\frac{\alpha^{3-\tau'}-1}{\alpha^{2-\tau'}-1}\right)\right] + A_{\rm f} s^{3/7}\left[\left(\frac{2-\tau'}{17/7-\tau'}\right)\left(\frac{\alpha^{17/7-\tau'}-1}{\alpha^{2-\tau'}-1}\right)\right]. \tag{5.4}$$

With $\tau' = \frac{15}{7}$ and $\alpha = 2^{1/8}$, we find

$$\Phi_s \simeq 0.174\,085 s + 1.018\,76 A_{\rm f} s^{3/7}. \tag{5.5a}$$

Similarly,

$$\Omega_s \simeq 0.348\,170 s + 1.018\,76 A s^{3/7} \tag{5.5b}$$

and

$$\mu_s \simeq 1.064\,39 A' s^{10/7} + 1.044\,51 B' s\,. \tag{5.5c}$$

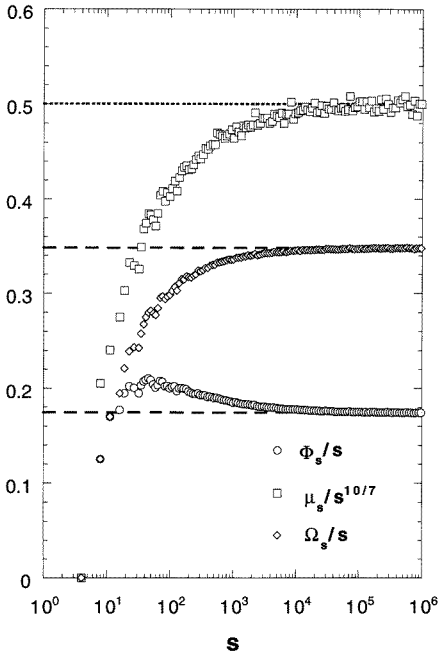

Figure 5. Binned values of Φ_s/s, $\mu_s/s^{10/7}$ and Ω_s/s. The broken horizontal lines indicate the exact asymptotic values and the dotted line is an estimated asymptotic value.

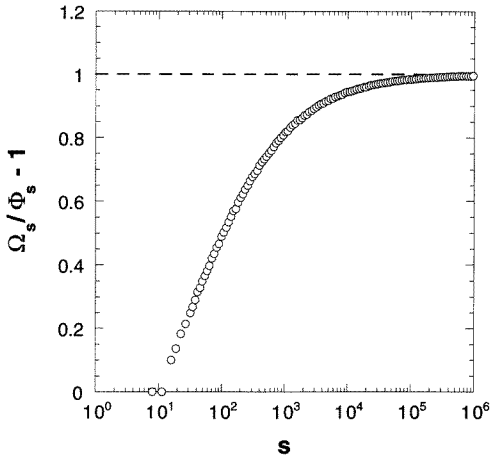

Figure 6. The ratio $(\Omega_s - \Phi_s)/\Phi_s$ plotted as a function of s, as a test of the conjecture made in equation (3.3).

We indeed observed that our data for Φ_s/s and Ω_s/s converge asymptotically to 0.174 085 and 0.348 170, respectively (figure 5). We were also able to check the conjecture made in equation (3.3) by plotting $(\Omega_s - \Phi_s)/\Phi_s$ as a function of s (figure 6). As conjectured, we find that this ratio converges asymptotically to one.

A finite-size estimator, $y_s = \log(\Phi_{2s}/\Phi_s)/\log 2$, was computed to determine the leading-order exponent of Φ_s, and similar estimators were used for Ω_s and μ_s. These estimators converge very slowly to constant values, so that the asymptotic regime is only reached for very long GOWs. To reduce the influence of the finite-size corrections, we plotted each estimator as a function of $1/s$ and extrapolated to $1/s \to 0$ (figure 7). For Φ_s and Ω_s, the extrapolated values are $y_\infty = 0.9985 \pm 0.0004$ and $y_\infty = 1.0006 \pm 0.0004$, respectively. The errors quoted here are solely due to the scatter in the data points. They do not take

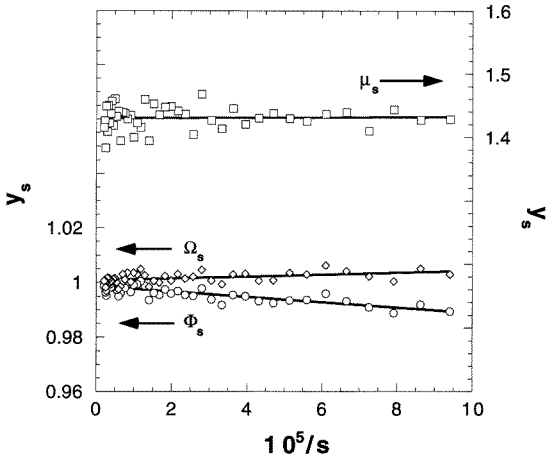

Figure 7. Extrapolation to $s \to \infty$ of the finite-size estimators y_s for the leading-order exponent of Φ_s, Ω_s and μ_s. The full lines are linear least-squares fits to the data points.

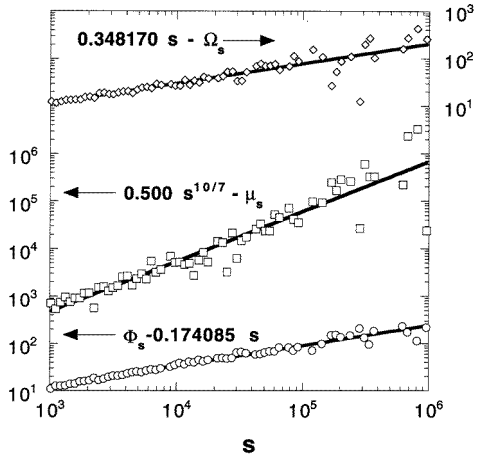

Figure 8. Numerical estimation of the leading-order correction terms for Φ_s, Ω_s and μ_s. The full lines are linear least-squares fits to the data points.

into account some other contributions to the uncertainty—the statistical error, for instance. Our results are thus in good agreement with the expected values, which are both equal to 1 (see equations (5.5*a*) and (5.5*b*)). A similar extrapolation gave $y_\infty = 1.430 \pm 0.004$ for μ_s, a result which is in excellent agreement with the value predicted by GB, $\frac{10}{7} = 1.4285\ldots$ (see equation (5.5*c*)). GB found an estimate of 1.60 ± 0.02 for this exponent that does not agree with their own prediction. The reason for this discrepancy is that GB only considered relatively small fragments. As a consequence, their estimate was biased by finite-size corrections. Finally, note that our data provide strong support for the validity of the scaling law (3.8) for $P_{\sigma,s}$.

Our next step was to check the values of the leading correction exponents given in (5.5). We computed the difference $\Phi_s - 0.174\,085s$ and plotted this quantity as a function of s (figure 8). A two-parameter fit of the data points to the form $\alpha_1 s^{-\alpha_2}$ gave $\alpha_1 = 0.66 \pm 0.07$ and $\alpha_2 = 0.43 \pm 0.01$. The data for $s < 10^3$ were not included in this fit because we observed that higher-order corrections are still significant in this range. Similarly, we obtained $\alpha_1 = 0.65 \pm 0.18$ and $\alpha_2 = 0.42 \pm 0.03$ from the data for $0.348\,170\, s - \Omega_s$ (figure 8). Both estimates of α_2 are in good agreement with the expected value, $\frac{3}{7} = 0.428\ldots$.

The exact asymptotic value of $\mu_s/s^{10/7}$ is not known. However, extrapolating this ratio

as $s \to \infty$, we were able to find the estimate $A' = 0.470 \pm 0.004$ (see figure 5). The data points for $0.500\ s^{10/7} - \mu_s$ were then fitted to the form $\alpha_1 s^{-\alpha_2}$ (figure 8). Here again, our estimate for the leading correction exponent, $\alpha_2 = 1.04 \pm 0.05$, is in good agreement with the expected value, unity. The corresponding estimate for the prefactor is $\alpha_1 = 0.35 \pm 0.17$.

As a by-product, rough estimates were obtained for the prefactors A_f, A, and B' (see equations (5)) which, to our knowledge, have not been computed previously. We find $A_f \simeq 0.65 \pm 0.07$, $A = -0.63 \pm 0.18$, and $B' = -0.33 \pm 0.16$.

6. Conclusions

In this paper, we introduced a model for the fragmentation of random porous objects resulting from chemical etching or combustion. In our model, the porous solid was represented by a bond percolation cluster on a square lattice and mass was removed only at the cluster's external perimeter.

We argued that the probability, $P_{\sigma,s}$, that the combustion of a cluster with perimeter s yields a fragment with perimeter σ, has the scaling form $P_{\sigma,s} = \sigma^{-\phi_H} G(\sigma/s)$, where G is a scaling function. The exponent ϕ_H is believed to be exactly $\frac{11}{7}$, and our numerical work strongly supports this belief. Our numerical work also supports the analytical work of Boughaleb and Gouyet on connection and disconnection events at diffusion fronts [4].

Using a relationship between our model and self-avoiding self-attracting loops on the Manhattan lattice, we argued that the average number of fragmenting bonds $\langle N_f(s) \rangle$ scales as $\frac{1}{6} s^{\lambda_H} + A_f s^{3/7}$ when s is large. Here the exponent λ_H is exactly equal to 1 and A_f is a constant. Our numerical work is in excellent agreement with this result.

Let us compare these results with the corresponding results in the GEF model of fragmentation. Let $P'_{\sigma,s}$ be the probability that the fragmentation of a percolation cluster of s bonds results in the formation of a fragment of σ bonds. GEF argued that $P'_{\sigma,s}$ obeys the scaling law $P'_{\sigma,s} = \sigma^{-\phi} H(\sigma/s)$ [1]. The exponent ϕ is believed to be exactly equal to $\frac{146}{91}$ [1, 13, 14], and so the values of ϕ_H and ϕ differ. This is not surprising, since other exponents describing the hull and bulk properties of two-dimensional percolation clusters differ as well. Finally, note that in the GEF model, the average number of fragmenting bonds scales as s^{λ}, where λ is exactly equal to 1 [14]. Thus, $\lambda_H = \lambda$.

The ratio of the number of external to internal perimeters proved to be a parameter that is extremely sensitive to hidden correlations in the pseudo-random number generator. The results we obtained by testing two standard generators are in excellent agreement with those found recently with specially designed tests.

So far, our simulations of the fragmentation of percolation hulls have been restricted to the two-dimensional case. Simulations in three dimensions, where the situation is still controversial [15, 16], are still needed.

Acknowledgments

We would like to thank J F Gouyet and B F Edwards for fruitful discussions.

References

[1] Gyure M F and Edwards B F 1992 *Phys. Rev. Lett.* **17** 2692
Edwards B F, Gyure M F and Ferer M 1992 *Phys. Rev.* A **10** 6252
[2] Ziff R M 1986 *Phys. Rev. Lett.* **56** 545

[3] Bradley R M 1990 *Phys. Rev.* A **41** 914
[4] Gouyet J F and Boughaleb Y 1989 *Phys. Rev.* B **40** 4760
[5] For a review of hull-generating walks, see Ziff R M 1989 *Physica* **38D** 377
[6] Gunn J M F and Ortuño M 1985 *J. Phys. A: Math. Gen.* **18** L1095
[7] Debierre J M and Bradley R M 1992 *J. Phys. A: Math. Gen.* **25** 335
[8] Prellberg T and Owczarek A L 1994 *J. Phys. A: Math. Gen.* **27** 1811
[9] Sapoval B, Rosso M and Gouyet J F 1985 *J. Physique Lett.* **46** 149
Rosso M, Gouyet J F and Sapoval B 1986 *Phys. Rev. Lett.* **57** 3195
[10] Vattulainen I, Ala-Nissila T and Kankaala K 1994 *Phys. Rev. Lett.* **73** 2513
[11] Press W H, Teukolsky S A, Vettering W T and Flannery B P 1992 *Numerical Recipes in C: the Art of Scientific Computing* (Cambridge: Cambridge University Press)
[12] Duplantier B and Saleur H 1987 *Phys. Rev. Lett.* **59** 539
[13] Gouyet J F 1990 *Physica* **168A** 581
[14] Gouyet J F 1993 *Phys. Rev.* B **47** 5446
[15] Gouyet J F 1992 *Physica* **191A** 301
[16] Roux S and Guyon E 1989 *J. Phys. A: Math. Gen.* **22** 3693